EPR and optical studies of Co^{2+} ions in MgO from local-spin-density molecular-orbital calculations

F. M. Michel-Calendini
Laboratoire de Physique des Solides, Université de Bourgogne, Boîte Postale 138, Batiment Mirande, F-21004 Dijon Cedex, France

K. Bellafrouh
Institute of Inorganic and Analytic Chemistry, Université de Fribourg, CH-1700 Fribourg, Switzerland

H. Chermette
Institut de Physique Nucléaire, Institut National de Physique Nucléaire et de Physique des Particules, Université Claude Bernard Lyon I, 43, Boulevard du 11 Novembre 1918 F-69622 Villeurbanne Cedex, France
(Received 21 December 1993; revised manuscript received 2 May 1994)

The EPR fine- and hyperfine-structure tensors of Co^{2+}, embedded in MgO, are calculated using a molecular-orbital approach within the density-functional-theory framework. Two methods, namely the multiple-scattering local-spin-density approximation and the linear combinations of atomic orbitals within local-spin-density approximations have been used for this purpose, leading to quite correct assignment of the optical spectrum and the EPR parameters. The pros and cons of both methods are underlined.

I. INTRODUCTION

The optical and EPR properties of the Co^{2+} ion trapped in MgO have been well studied experimentally for a long time. The ground state is a $^4T_1$ orbital triplet and the fine-structure factor g is equal to 4.28. In early work, Low[1] roughly estimated the crystal field (hereafter denoted CF) parameter Dq from absorption results. More complete CF data have been devised from absorption and fluorescence spectra by several authors.[2–7] Raman scattering yields the spin energy levels inside the ground-state term.[6] A more recent work[8] reports absorption spectra from 15 K to room temperature and identifies some zero-phonon lines in the absorption bands.

On the other hand, the theory of fine and hyperfine structure for a d^7 ion in an octahedral environment is extensively developed in reference books,[9–11] but the problem of knowing how the impurity disturbs the initial host is still a subject of controversy.

Compared to this abundance of experimental data, electronic structure calculations bearing on a system like MgO:Co^{2+} are rather incomplete. A spin-polarized Hartree-Fock calculation has been reported for the CoO_6^{10-} cluster[12] but a complete derivation of term energies and EPR parameters from electronic structure results has not yet been attempted.

The purpose of the present paper is to provide such theoretical investigations using molecular-orbital calculations. Calculations are carried out using the density-functional approach.[13,14] In this work both the multiple-scattering local-spin-density[15] (MS LSD) method and linear combination of Gaussian-type orbitals within the local-spin-density approximation (LCGTO-LSD) (Ref. 16) methods have been applied to cubic CoO_6^{10-} clusters.

The MS $X\alpha$ method has been used successfully for a long time to describe the electronic properties of such transition-metal ions in oxides[17,18] and in particular for cobalt ions in perovskite-type compounds.[19] The derivation of CF parameters, term energies, and EPR properties has also been attempted for d^3 and d^5 ions in some oxides.[20–22] The LCGTO LSD approach, more demanding in computational resources, has been generally used for neutral complexes and to a lesser extent for heavily charged clusters; some recent works in this way were encouraging, notably because of the accuracy of total-energy calculations, leading to the possibility of simulating the local structure around the transition-metal ion.[21,22] Thus it appears worthwhile to compare the results provided by both LSD approaches for the electronic structure, the optical, and the EPR properties of Co^{2+} in MgO, in relation to the well-established experimental data. Most of the parameters involved in EPR and crystal-field properties are obtained from these calculations: the spin-orbit coupling constant ζ_{3d}, s spin densities $\rho\uparrow-\rho\downarrow$ at the nucleus, $\langle r^{-3}\rangle_{3d}$ integrals, and CF and Racah parameters B and C. Term energy calculations are carried out using the intermediate CF scheme of Tanabe and Sugano,[9] with the d^7 electrostatic matrices. The ligand-field multiplets and the associated determinantal functions provide the fine and hyperfine constants.

The paper is divided as follows. Section II describes the theoretical background relevant to each LSD method; the molecular-orbital eigenvalue diagrams are reported and discussed. Section III reports the determination of Racah and ζ_{3d} parameters from MS LSD methods and the term-energy calculations. Section IV concerns the evaluation of g and A tensors. The covalency is discussed from these results. Each section includes compar-

isons to other theoretical and experimental data. A general conclusion is given in Sec. V.

II. LOCAL-SPIN-DENSITY METHODS APPLIED TO CoO_6 CLUSTERS

The basis of the density-functional theory, which allows the determination of electronic properties of molecular systems, is well described in several papers (e.g., Ref. 13) and does not deserve extensive comments.

Ground-state calculations are carried out for Co^{2+}, $S=\frac{3}{2}$, embedded in a CoO_6^{10-} cluster with a metal-ligand distance of 2.1 Å, representative of the MgO length in an undoped crystal. This work is in the spirit of earlier calculations reported in the past[16] for other cubic oxides with distances of 1.95 and 2 Å using the MS $X\alpha$ method, but goes beyond these works because of the use of the more accurate linear combination of atomic orbitals (LCAO) approach for the energy determination.

A. MS LSD method

The MS LSD method is well documented (e.g., Refs. 15 and 19 and references therein) and only typical details are reported here. The cluster is divided into outer sphere (OS), inner sphere (IS), and atomic spheres; standard concepts such as the touching-sphere requirement and the Norman rule[23] are used for the sphere radii. A Watson sphere surrounds the cluster and bears a charge of 10.5 to simulate roughly the cluster environment. The sphere radii are $R_{Co}=2.1$ a.u., $R_O=1.869$ a.u., and $R_{OS}=R_W=5.838$ a.u. The exchange-correlation potential is treated by the Vosko, Wilk, and Nusair (VWN) approximation.[24] The relativistic option yields the spin-orbit coupling constant ζ_{3d}.[25] The spin densities are simply extracted from the self-consistent field (SCF) spin-orbital sets as well as the $\langle r^{-3}\rangle_{3d}$ integrals and the spin-orbit parameters for which a slightly different value is obtained for each orbital. For these two last parameters, a weighted averaged value is calculated to obtain the parameters introduced in term-energy and EPR calculations.

B. LSD LCGTO calculations

We also worked in the framework of the linear combination of Gaussian-type orbitals with the DEMON code developed by Saint Amant.[26] We used the (631/41/1*) orbital basis set for O developed by Godbout *et al.*[27] and a (6332*/531*/4**) one for Co. This latter is just the one established by Godbout *et al.* from which the most diffuse *d* function has been removed. It has already been observed that the inclusion of too diffuse functions may yield erroneous description of ions in crystalline hosts.[28] This effect, which may look contrary to the scheme of the variational theorem, is related to basis-set superposition errors occurring in systems with negative ions like O^{2-}; in other words, it would be necessary to compensate the metal diffuse orbital by one or two very diffuse functions on the oxygen atom. The Co(5,5;5,5) and O(4,4;4,4) auxiliary basis states are taken from Ref. 27. The exchange-correlation potential is restricted to the local approximation (LSD) provided by the VWN formula.[24]

C. Eigenvalue diagrams

The eigenvalues relevant to the different orbitals are listed in Table I for both MS and LCGTO calculations. Several important remarks can be drawn from this table. First of all, a general upward shift of about 50 eV is observed for the LCGTO vs the MS eigenvalues. This shift is evidently due to the use of the Watson sphere approxi-

TABLE I. LSD monoelectronic eigenvalues in MgO:Co^{2+} (occupation numbers in parentheses, energies in eV).

	MSLSD		LCGTO LSD	
	Spin up	Spin down	Spin up	Spin down
			inner levels	
Co 1*s*	−7495.0 (1)	−7495.0 (1)	−7440.0 (1)	−7440.0 (1)
Co 2*s*	−875.2 (1)	−876.7 (1)	−822.2 (1)	−821.7 (1)
Co 2*p*	−760.3 (3)	−761.5 (3)	−707.4 (3)	−706.3 (3)
O 1*s*	−504.5 (6)	−504.6 (6)	−452.4 (6)	−452.3 (6)
Co 3*s*	−93.6 (1)	−93.4 (1)	−41.2 (1)	−38.2 (1)
Co 3*p*	−59.3 (3)	−62.1 (3)	−6.9 (3)	−4.0 (3)
O $2sa_{1g}$	−21.2 (1)	−21.3 (1)	32.7 (1)	32.8 (1)
O $2st_{1u}$	−20.7 (3)	−20.8 (3)	33.1 (3)	33.1 (3)
O $2se_g$	−20.6 (2)	−20.7 (2)	33.2 (2)	33.3 (2)
			O 2*p* valence band (extrema values)	
O $2pa_{1g}$	−8.1 (1)	−8.3 (1)	44.8 (1)	45.0 (1)
O $2pt_{1g}$	−6.0 (3)	−6.1 (3)	47.6 (3)	47.6 (3)
			antibonding levels	
Co $3dt_{2g}$	−5.45 (3)	−3.32 (2)	50.11 (3)	52.54 (2)
Co $3de_g$	−3.83 (2)	−2.21 (0)	51.11 (2)	53.35 (0)
Co $4sa_{1g}$	−3.98 (0)	−3.94 (0)	56.89 (0)	57.28 (0)
Co $4pt_{1u}$	−2.73 (0)	−2.68 (0)	57.62 (0)	57.70 (0)

mation in the MS LSD calculation, absent in the LCAO approach.

Secondly, the LCGTO hierarchy of Co $3d$, Co $4s$, and Co $4p$ levels is the following: the $4s$ states lie about 3 eV above the $3d$ ones and the $4p$ states are slightly higher than the $4s$ ones. All of them keep a good atomic character, contrary to MS results where $4s$ and $4p$ orbitals are highly delocalized in the OS region (Rydberg states) with corresponding levels lying below or between the $3d$ ones. The covalency degree of antibonding $3d$ orbitals deserves some comments as it will be used further in the EPR and optical calculations. Population analyses are performed in a classical Mulliken analysis for the LCAO approach while in the MS LSD approach a distribution of IS and OS densities into atomic spheres is made. The percentages of $3d$ orbital character are the following:

$t_{2g}\uparrow$: 85.0 (MS), 91.6 (LCGTO);

$t_{2g}\downarrow$: 58.0 (MS), 95.3 (LCGTO);

$e_g\uparrow$: 91.0 (MS), 78.5 (LCGTO);

$e_g\downarrow$: 57.0 (MS), 88.1 (LCGTO).

We notice the relative stability of the covalency in LCAO calculations, contrary to the multiple-scattering approach, which exhibits a strong disparity between fully occupied, partially occupied, or empty levels, due to the outer-sphere delocalization of the last, which makes questionable the meaning of a population analysis for this type of orbital. Moreover, the nominal ionicity of Co and O ions appears more realistic in DEMON than in MS results; indeed, the cluster charges are found equal to $[Co^{0.74}O^{1.79-}]^{10-}$ (MS) and $[Co^{1.88}O^{1.98-}]^{10-}$ (LCGTO). This is a common feature for MS $X\alpha$ results to yield weaker ionicities than other methods.

The main disappointment in LCGTO calculations is the apparent wrong positions of the antibonding $3d$ levels relatively to the O $2p$ valence-band (VB) top. This is illustrated in Fig. 1, where t_{2g} and e_g antibonding levels are plotted relative to the O $2p$ t_{1g} one, chosen as reference (zero-energy) level, and representing the O $2p$ VB top, as stated earlier.[19] The LCGTO levels are shifted upward almost uniformly by 2 eV compared to the MS ones, shifting up by the same amount all the charge-transfer transitions. This is not a drawback as far as the stability of the Co^{2+} ion in MgO is concerned, since the O $2p$–Mg $3s$ gap amounts to ca. 7 eV, but it contradicts the experimental assignment of an intense absorption band at 17 125 cm^{-1} to charge transfer.[8] Indeed, the O $2p$–Co $3d$ charge-transfer band is predicted to lie around 40 000 cm^{-1} in LCGTO calculations compared to 22 500 cm^{-1} in MS ones. This MS result is only slightly overestimated compared to experiment, as was already noticed in MS $X\alpha$ data for cobalt ions in perovskites.[19]

More disturbing is that similar LCAO calculations carried out on CoO_6^{10-} clusters with 2 and 1.95 Å metal-ligand distances, assumed to represent Co^{2+} in $SrTiO_3$ and $BaTiO_3$ perovskite hosts, would predict this ion to be unstable in these crystals, while it is well identified experimentally. Indeed, the relevant eigenvalue diagrams

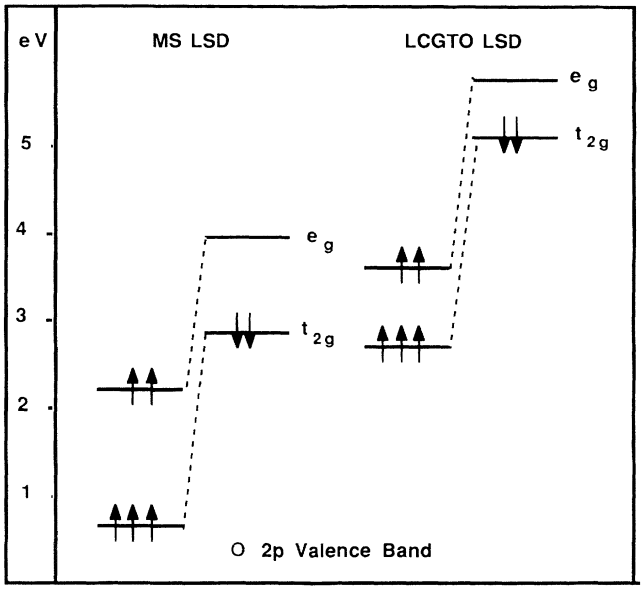

FIG. 1. Eigenvalues of the antibonding $3d$ levels of Co^{2+} in MgO (O $2p$ VB is the O $2p$ t_{1g} level of Table I).

present few differences with the ones pictured in Fig. 1; on the other hand, the LCGTO calculations carried out on suitable TiO_6^{8-} clusters depicting the undoped crystals (as described in $X\alpha$ calculations[17]) yield a conduction-band edge Ti $3dt_{2g}$ localized at about 3.5 eV above the O $2pt_{1g}$ level; so the Co $3d$ occupied level would lie in the conduction band of these crystals, making Co^{2+} unstable. More accurate calculations of charge-transfer energies using the total-energy difference between excited- and ground-state configurations yield worse results by increasing the O $2p$–Co$t_{2g}\downarrow$ or O $2p$–Co$e_g\downarrow$ transition energies. The MS results predict more correct positions of the Co antibonding levels inside the band gap.[19] It is remarkable that both MS and LCGTO results lead to the same values (around 3.5 eV) for the O $2pt_{1g}$ to Ti $3dt_{2g}$ splitting in the TiO_6^{8-} clusters. Furthermore, earlier LCGTO calculations on Cr^{3+}, Mn^{4+}, and Fe^{3+} show that the positions of the impurity levels inside the perovskite band gaps are similar to the ones obtained by the MS approach. It was shown that the positions of the $3d$ antibonding levels along the $3d$ ion sequence appear correctly describe in the MS $X\alpha$ frame-

TABLE II. Crystal-field parameters (cm^{-1}) in MgO:Co^{2+}. (Expt. 1 from Ref. 10, Expt. 2 from Ref. 4, Expt. 3 from Ref. 5, and Expt. 4 from Ref. 8.)

	MS	LCGTO	Expt. 1	Expt. 2	Expt. 3	Expt. 4
Dq	968	850	840	930	895	880
B	987	987	800	840	800	780
C	3605	3605	2986	3700	3750	3510
ζ_{3d}	516	516	536	475	500	475

work.[17]

The absence of a Madelung potential in our LCAO approach could be responsible for most of the discrepancy for heavily charged clusters like CoO_6^{10-}. Its introduction, at least via a description of the ionic host by a net point charge, is in progress. The GTO wave functions may also be questioned. Indeed, very recent LSD calculations[28] using the ADF code[29] (including Slater-type orbitals, no Madelung potential modeling, and the VWN approximation) for the same cluster predict antibonding Co level positions in complete agreement with the experimental trends.

III. TERM-ENERGY CALCULATIONS

Optical spectra and EPR parameters are obtained as follows. B and C are evaluated from MS LSD MO calculations as described previously.[20,30,31] The CF strength Dq is obtained from eigenvalue diagrams relevant either to MS or to LCGTO calculations. For B and C, we use (i) the t_{2g} to e_g energy difference in the non-spin-polarized Slater transition state $t_{2g}^{4.5}e_g^{2.5}$; (ii) the energy difference between the $e_g\downarrow$ and $t_{2g}\downarrow$ eigenvalues in the ground-state configuration $t_{2g}\uparrow^3 e_g\uparrow^2 t_{2g}\downarrow^2$.

For the latter, 10Dq is estimated (i) from the total-energy difference between the configurations $t_{2g}\uparrow^3 e_g\uparrow^2 t_{2g}\downarrow^2$ and $t_{2g}\uparrow^3 e_g\uparrow^2 t_{2g}\downarrow^1 e_g\downarrow^1$ or from the previous option (ii). Theoretical Dq values gathered in Table II are obtained from option (i) and will be retained further in theoretical term calculations. Indeed, the Dq values obtained from (ii) are substantially weaker: 894 cm^{-1} (MS) and 677 cm^{-1} (LCGTO) and must be discarded compared to literature experimental data (denoted Expt. 1–Expt. 4 in Table II). The B and C theoretical values are the MS LSD ones.

The absorption spectrum of $MgO:Co^{2+}$ was reported by Low[1] and approximately fitted with $Dq=960$ cm^{-1}. Later absorption and fluorescence spectra[2–4] were fitted using the Expt. 2 parameter set (the authors of Ref. 4 used $Dq=900$ cm^{-1} instead of 930 cm^{-1} in the Expt. 2 set). The possible reduction of the spin-orbit coupling constant by the dynamic Jahn-Teller effect is discussed in Ref. 4. Raman scattering experiments allow one to attribute an experimental peak at 935.7 cm^{-1} to the E' to $^2U'$ transition inside the ground state. The parameter set Expt. 3 stems from the fit of magnetic circular dicroism experiments.[5] Recent absorption and fluorescence measurements[8] show two bands peaking at 8500 and 19 500

TABLE III. Multiplet energies (cm^{-1}) of Co^{2+} in MgO.

State		MS	LCGTO	Fit[a]	Experimental positions	
$1\,^4T_1$	E'	0	0	0		
	U'	343	344	329		330[b]
	U'	893	898	859	935.7[c]	890[b]
	E''	990	994	951		930[b]
$1\,^4T_2$	E'	8 950	8 530	8 353	9 000[d]	8 141[e]
	U'	8 996	8 565	8 375	8 152[f]	8 168[e]
	U'	9 096	8 659	8 465	8 166[f]	8 208[e]
	E''	9 285	8 866	8 678	8 203[f]	8 500[e]
$1\,^2E$	U'	8 743	9 225	8 926	8 045[f]	
$1\,^2T_1, 1\,^2T_2$	U'	16 394	16 339		16 000[a]	15 812[e]
$1\,^4A_2$	U'	17 026	17 012	16 514	17 000[a]	
	U'	18 782	17 924	17 461		
$2\,^2T_1, 2\,^2T_2$	E', E''	16 926	16 946	16 296		
	E', E''	17 224	17 012	16 747		
$2\,^4T_1$	U'	22 393	22 028	19 030	20 000[d]	19 500[e]
$^4T_2$	U'	23 172	22 908	19 169	20 000[d]	
	E', E''	22 405	22 016	19 164	20 000[d]	
	E', E''	23 202	22 830	19 558	20 000[d]	
$3\,^2T_1$	U'	21 253	21 123	20 730	20 000[d]	
	E'	21 107	21 746	20 813	20 000[d]	
$^2A_1$	E'	24 009	23 630	23 001	23 000[a]	
$3\,^2T_2$	U'	26 332	28 018	24 930	25 000[a]	
	E''	26 078	25 753	24 696	25 000[a]	
$4\,^2T_1$	U'	27 615	27 204	25 958	27 000[a]	
	E'	27 664	27 243	26 037	27 000[a]	
$2\,^2E$	U'	29 582	29 159	27 869	28 000[a]	

[a]Reference 5.
[b]Reference 6.
[c]Reference 7.
[d]References 1 and 5.
[e]Reference 8.
[f]Reference 4.

TABLE IV. Relations between terms and configurations for d^7 ions in cubic symmetry.

Term	Configuration	Term	Configuration
$^2A_1$	$e^3t_2^4$	$^2A_2$	$e^3t_2^4$
$1\,^2E$	$e^1t_2^6$	$2\,^2E$	$e^3t_2^4$
$3\,^2E$	$e^3t_2^4$	$4\,^2E$	$e^4t_2^3$
$1\,^2T_1$	$e^2t_2^5$	$2\,^2T_1$	$e^2t_2^5$
$3\,^2T_1$	$e^3t_2^4$	$4\,^2T_1$	$e^3t_2^4$
$5\,^2T_1$	$e^2t_2^3$		
$1\,^2T_2$	$e^2t_2^5$	$2\,^2T_2$	$e^2t_2^5$
$3\,^2T_2$	$e^3t_2^4$	$4\,^2T_2$	$e^3t_2^4$
$5\,^2T_2$	$e^4t_2^3$		
$1\,^4T_1$	$e^2t_2^5$	$2\,^4T_1$	$e^3t_2^4$
$^4T_2$	$e^3t_2^4$	$^4A_2$	$e^4t_2^3$

cm^{-1} and let us identify three zero-phonon lines at 8141, 8168, and 8208 cm^{-1} as spin levels of the $^4T_2$ band; these spectra are interpreted with the parameter set Expt. 4 of Table II. The set Expt. 1 is proposed in Ref. 10 to fit the EPR data.

Term energies are then deduced from d^7 matrix calculations as described earlier for d^3 and d^5 ions[21,22] using the LSD and the various Expt. i ($i=1-4$) sets. The experimental or fitted spectra are compared to the theoretical MS and LCGTO term energies in Table III using the relations between the term assignments and the configurations displayed in Table IV.

Beyond the lowest orbital terms, the examination of eigenvectors relevant to each state shows that the spin-orbit coupling effects appreciably mix the spin components of the initial ligand-field states. Accordingly, the orbital character indicated for each term is the leading one. When this is not possible, the different main orbital components are given. This yields slightly different term assignments from the ones given in previous works.[5,8]

We see that the LCGTO multiplets match well the optical structure found in the optical bands. In particular, Dq extracted from LCGTO results is quite good while the MS LSD one looks slightly overestimated. The spin-orbit coupling constant appears also slightly overestimated when the theoretical and experimental positions of the spin states are compared. The best fit corresponds to a reduction of the theoretical ζ_{3d} by a factor amounting to 0.96, corresponding to the estimated covalency of the metal-ligand bonds depicted in the previous section. It has been stated previously[4,5] that the Dq/B ratio for Co^{2+} in MgO corresponds to the crossover region between the $1\,^2E$ and the $^4T_2$ levels ($Dq/B=1.1$).[9] So a little variation in the CF parameters may reverse the order of these two levels. This is clearly evident from the parameter set of Ref. 4 (Expt. 2) where $^2T_2$ lies 103 cm^{-1} below $^4T_2E'$, while the fit performed with the Expt. 3 set pushes it about 500 cm^{-1} above $^4T_2E'$ (see Table III). It is clear that it is mainly the effect of Dq variation, as evidenced from the MS and LCGTO results which differ only in the Dq value. A larger Dq value (969 cm^{-1} as in the MS set) pulls the ^2E level 200 cm^{-1} below the lowest $^4T_2$ state, while a slightly smaller one (850 cm^{-1} as in LCGTO) pushes it 700 cm^{-1} above the upper $^4T_2$ one. This points out the difficulty of performing a correct assignment of terms in a CF experimental spectrum, even for a simple case such as Co^{2+} in a cubic environment.

IV. FINE- AND HYPERFINE-STRUCTURE PARAMETER CALCULATIONS

The theory of fine- and hyperfine-structure tensors for a d^7 ion, $S=\frac{3}{2}$ was developed extensively by Abragam and Pryce,[32] and has been recalled in many references;[9,10] the main features are as follows.

Co^{2+} in MgO experiences a weak ligand field (Dq/B less than 2 in the Tanabe and Sugano diagram) with a ligand-field fundamental wave function $|\Phi\rangle=\varepsilon|\phi_1\rangle+\tau|\phi_2\rangle$ built upon the eigenvectors associated with the two $^4T_1$ states (see Table IV) denoted $|\phi_1\rangle=|1\,^4T_1\phi_0\rangle$ and $|\phi_2\rangle=|2^4T_1\phi_0\rangle$, with

$$|\phi_0\rangle=\sqrt{\tfrac{1}{2}}|\tfrac{3}{2},-1\rangle-\sqrt{\tfrac{1}{3}}|\tfrac{1}{2},0\rangle+\sqrt{\tfrac{1}{6}}|-\tfrac{1}{2},1\rangle\ .$$

An α term, defined by $\alpha=-\frac{3}{2}\varepsilon^2+\tau^2$, may be introduced to estimate the degree of mixing between the two $^4T_1$ components. The actual spin wave function $|\Phi\rangle$ relevant to the ground $|1\,^4T_1E'\rangle$ doublet involves a further contribution of the $^4T_2$ state, due to spin-orbit coupling effects. For instance, term-energy calculations with the LCGTO CF set lead to

$$|\Phi\rangle=0.955|1\,^4T_1\phi_0\rangle+0.262|2\,^4T_1\phi_0\rangle$$
$$+0.146|1\,^4T_2\phi_0\rangle\ .$$

TABLE V. Fine- and hyperfine-structure parameters in $MgO:Co^{2+}$.

Data set	MS	LCGTO	Expt. 1	Expt. 2	Expt. 3	Expt. 4
α	1.329	1.335	1.402	1.355	1.357	1.355
k	0.91[a]	0.95	0.82	0.97	0.96	0.96
g	4.238	4.301	4.280	4.280	4.280	4.280
$\rho\uparrow-\rho\downarrow$ (a.u.)	−0.366		−0.586[b]			
$\langle r^{-3}\rangle_{3d}$ (a.u.)	4.956		5.12			
χ	0.206		0.320			
A (MHz)	339		290			

[a]From the covalency of the $t_{2g}\downarrow$ orbital only.
[b]From $\chi=0.32$ a.u. (free-ion value).

The α parameter may be estimated by neglecting the third contribution and normalizing the two former ones, leading to $\alpha(\text{LCGTO}) = -1.325$.

It may also be approximated from the energy difference δ between the first quartet $|1\,^4T_1U'\rangle$ and the ground doublet $|1\,^4T_1E'\rangle$ through

$$\delta = -\alpha\zeta_{3d}/2 \ .$$

This yields $\alpha(\text{LCGTO}) = -1.33$.

The spin Hamiltonian takes the usual form,

$$H = \beta \mathbf{g}\cdot\mathbf{H}\cdot\mathbf{S} + \mathbf{A}\cdot\mathbf{I}\cdot\mathbf{S} \ .$$

The g factor is obtained from the equation

$$\mathbf{H}\cdot\mathbf{g}\cdot\mathbf{S}|\Phi\rangle = \mathbf{H}(g_l\mathbf{l} + g_S\mathbf{S})|\Phi\rangle$$

with $g_l = -1.5k$ and $g_S = 2$, with an orbital reduction factor k to account for the metal-ligand covalency.

The fine-structure factor g and the hyperfine one A are related to the $\langle r^{-3}\rangle_{3d}$, $\rho\uparrow - \rho\downarrow$, and α parameters through the relations[9]

$$X = (4\pi/2S)(\rho\uparrow - \rho\downarrow) \ ,$$

$$\chi\langle r^{-3}\rangle_{3d} = -\tfrac{2}{3}X \ ,$$

$$A = 2g_n\beta\beta_n\langle r^{-3}\rangle_{3d}\{-\tfrac{2}{3}\alpha - \tfrac{5}{3}\chi - \tfrac{1}{63}(8+6\alpha)\} \ ,$$

with $\beta_n = 1.322$ for Co (Ref. 10). The quantities $(\rho\uparrow - \rho\downarrow)$ and $\langle r^{-3}\rangle_{3d}$ are averaged from the integrals obtained in MS spin-polarized calculations as outlined in Sec. II A.

Fine-structure, hyperfine-structure, and α parameters relevant to MS, LCGTO, and Expt. 2–4 parameter sets are compared to fitted or experimental values Expt. 1 in Table V. For sets Expt. 2–4, we choose the orbital reduction factor k in order to obtain $g = 4.280$. The LCGTO g constant appears rather good while the MS one is underestimated, due to the weaker MS k value. The LSD integrals included in hyperfine calculations are near the Hartree-Fock free-ion values of Expt. 1 and the theoretical estimation of A appears correct.

V. CONCLUSION

The present method has allowed us to investigate the predictive power of two methods based on density-functional theory for the estimation of the electronic structure of the Co^{2+} ion embedded in a typical oxide crystal host, namely, MgO. Thus, significant optical and EPR data are obtained theoretically from monoelectronic eigenvalues. The two approaches lead to nearly similar results, as expected, which are in relative agreement with experiment. Nevertheless, the MS LSD approach provides a better description of the positions of the antibonding Co $3d$ levels above the O $2p$ valence band, while the LCGTO approach lacks here an embedding scheme modeling the crystal host.

These kinds of calculations, via small-cluster representations, can be used as a probe of the local structure of any $3d$ impurity center in a crystal.

[1] W. Low, Phys. Rev. **109**, 256 (1958).
[2] R. Pappalardo, D. L. Wood, and R. Linares, J. Chem. Phys. **35**, 2041 (1961).
[3] A. D. Liehr, J. Phys. Chem. **67**, 1314 (1963).
[4] J. E. Ralph and M. G. Townsend, J. Chem. Phys. **48**, 149 (1968).
[5] A. J. Mann and P. J. Stephens, Phys. Rev. B **9**, 863 (1974).
[6] L. T. Peixoto and M. E. Foglio, Phys. Rev. B **32**, 2596 (1985); *ibid.* **33**, 2842 (1986).
[7] H. Guha, Phys. Rev. B **21**, 5808 (1980).
[8] H. Manaa, Ph.D. thesis, Université de Lyon, 1991.
[9] J. S. Griffith, *Theory of Transition Ions* (Cambridge University, Cambridge, England, 1981).
[10] A. Abragam and B. Bleaney, *Résonance Paramagnetique des Ions de Transitions* (Presses Universitairs de France, Paris, 1971).
[11] C. J. Ballhausen, *Introduction to Ligand Field Theory* (McGraw-Hill, New York, 1956).
[12] D. L. Klein, G. T. Suratt, and A. B. Kunz, J. Phys. C **12**, 3913 (1979).
[13] R. G. Parr and W. Yang, *Density Functional Theory of Atoms and Molecules* (Oxford University, New York, 1989).
[14] T. Ziegler, Chem. Rev. **91**, 651 (1991).
[15] H. Chermette, New J. Chem. **126**, 1081 (1992).
[16] D. R. Salahub, in *Applied Quantum Chemistry*, edited by V. H. Smith, H. F. Schaefer, and K. Morokuma (Reidel, Dordrecht, 1986), p. 185; D. R. Salahub, Adv. Chem. Phys. **15**, 447 (1987).
[17] F. M. Michel-Calendini, H. Chermette, and J. Weber, J. Phys. C **13**, 1427 (1981).
[18] F. M. Michel-Calendini, P. Moretti, and H. Chermette, J. Chim, Phys. **84**, 835 (1987).
[19] F. M. Michel-Calendini and P. Moretti, Phys. Rev. B **27**, 763 (1983).
[20] K. Bellafrouh, H. Chermette, C. Daul, A. Goursot, and F. Michel-Calendini, J. Chim. Phys. **86**, 933 (1989).
[21] F. Michel-Calendini and C. Daul, Ferroelectrics **125**, 277 (1992).
[22] K. Bellafrouh, C. Daul, and F. Michel-Calendini, New J. Chem, **16**, 1123 (1992).
[23] J. G. Norman, Jr., J. Chem. Phys. **61**, 4630 (1974).
[24] S. H. Vosko, L. Wilk, and M. Nusair, Can. J. Phys. **58**, 1200 (1980).
[25] M. Morin, D. R. Salahub, S. Nour, C. Mehadji, and H. Chermette, Chem. Phys. Lett. **159**, 472 (1989).
[26] A. Saint Amant, Ph.D. thesis, University of Montreal, 1991.
[27] N. Godbout, D. R. Salahub, J. Andzelm, and E. Wimmer, Can. J. Chem. **70**, 560 (1992).
[28] F. Michel-Calendini (unpublished).
[29] ADF code, Department of Theoretical Chemistry, Vrije Universiteit, De Boelaan 1083, 1081 HV Amsterdam, The Netherlands.
[30] A. Goursot and C. Daul, Int. J. Quantum Chem. **29**, 779 (1986).
[31] K. Bellafrouh, Ph.D. thesis Université de Lyon, 1990.
[32] A. Abragam and M. H. L. Pryce, Proc. R. Soc. London Ser. A **206**, 173 (1951).